



**GALACTO-OLIGOSACCHARIDES AND LACTULOSE AS
PROTECTANTS AGAINST DESICCATION OF LACTOBACILLUS
DELBRUECKII SUBSP. BULGARICUS**

Journal:	<i>Biotechnology Progress</i>
Manuscript ID:	BTPR-14-0068.R1
Wiley - Manuscript type:	Research Article
Date Submitted by the Author:	01-Jul-2014
Complete List of Authors:	Santos, Mauricio; Center for Research and Development in Food Cryotechnology (CIDCA CCT-La Plata), Araujo-Andrade, Cuauhtémoc; Universidad Autónoma de Zacatecas, Unidad Académica de Física Esparza-Ibarra, Edgar; Universidad Autónoma de Zacatecas, Unidad Académica de Biología experimental Tymczyszyn, E; Center for Research and Development in Food Cryotechnology (CIDCA CCT-La Plata), Gomez-Zavaglia, Andrea; Center for Research and Development in Food Cryotechnology (CCT-CONICET La Plata),
Keywords:	Lactobacillus delbrueckii subsp. bulgaricus, Desiccation, Galacto-oligosacharides, Near infrared spectroscopy, Damage

SCHOLARONE™
Manuscripts

1
2
3 **1 GALACTO-OLIGOSACCHARIDES AND LACTULOSE AS PROTECTANTS**
4
5 **2 AGAINST DESICCATION OF *LACTOBACILLUS DELBRUECKII* SUBSP.**
6
7 **3 *BULCARICUS***
8
9
10
11

12 Mauricio I. Santos^a, Cuauhtémoc Araujo-Andrade^b, Edgar Esparza-Ibarra^c, Elizabeth
13 Tymczyszyn^a and Andrea Gómez-Zavaglia^{a1}
14
15
16
17
18
19

20 ^a *Center for Research and Development in Food Cryotechnology (CCT-CONICET La Plata), RA-1900,*
21 *Argentina*

22 ^b *Unidad Académica de Física. Universidad Autónoma de Zacatecas. Zacatecas, MX 98000 Mexico.*

23 ^c *Unidad Académica de Biología experimental. Universidad Autónoma de Zacatecas. Zacatecas, MX 98000*
24 *Mexico*
25
26
27
28
29
30
31
32
33
34
35
36
37
38
39
40
41
42
43
44
45
46
47
48
49
50
51
52
53
54
55

56
57 ¹Corresponding author. Tel.: +54 221 4254853; Fax: +54 221 4249287
58 E-mail address: angoza@qui.uc.pt
59
60

1
2
3 **Abstract**

4 *Lactobacillus delbrueckii* subsp. *bulgaricus* CIDCA 333 was dehydrated on desiccators containing silica gel in
5 the presence of 20% w/w of two types of galacto-oligosaccharides (GOS Biotempo and GOS Cup Oligo H-70®)
6 and lactulose, until no changes in water desorption were detected. After rehydration, bacterial growth was
7 monitored at 37 °C by determining: a) the absorbance at 600 nm; b) the near infrared spectra (NIR). Principal
8 Component Analysis (PCA) was then performed on the NIR spectra of samples dehydrated in all conditions. A
9 multiparametric flow cytometry assay was carried out using carboxyfluorescein diacetate and propidium iodide
10 probes to determine the relative composition of damaged, viable and dead bacteria throughout the growth
11 kinetics.

12 The absorbance at 600 nm and the position of the second derivative band at ~1370 nm were plotted against the
13 time of incubation. The efficiency of the protectants was GOS Biotempo > GOS Cup Oligo H-70® > lactulose.

14 The better protectant capacity of GOS Biotempo was explained on the basis of the lower contribution of
15 damaged cells immediately after rehydration (t=0). PCA showed three groups along PC1, corresponding to the
16 lag, exponential and stationary phases of growth, which explained 99% of the total variance. Along PC2, two
17 groups were observed, corresponding to damaged or viable cells.

18 The results obtained support the use of NIR to monitor the recovery of desiccated microorganisms in real time
19 and without the need of chemical reagents. The use of GOS and lactulose as protectants in
20 dehydration/rehydration processes was also supported.

21
22
23
24
25
26
27
28
29
30
31
32
33
34
35
36
37
38
39 **Keywords:** *Lactobacillus delbrueckii* subsp. *bulgaricus*; Desiccation; Galacto-oligosachharides; Lactulose;
40 Near infrared spectroscopy; Multiparametric flow cytometry; Damage; Viable cells.

42 INTRODUCTION

43 The importance of lactic acid bacteria in the elaboration of dairy products underlines the
44 necessity of an adequate preservation. The decrease of water activity is responsible for cell damage
45 during preservation and lipid membranes are the first targets of dehydration injury. This loss of water
46 is responsible for both bacteria damage and loss of viability, both of them finally delaying the
47 fermentation processes [1,2]. Therefore, the use of protective compounds is crucial to avoid damage
48 during dehydration [3-8]. In the last years certain sugars, like galacto-oligosaccharides (GOS) and
49 lactulose have demonstrated a good protective properties [7,8].

50 Two hypotheses were proposed to explain the protectant capacity of sugars: vitrification and
51 capacity to replace water molecules [9,10]. The vitrification hypothesis explains protection mediated
52 by sugars on the basis of their capacity to form glassy states [sugars with high vitreous transition
53 temperatures (T_g) are better protectants because they contribute to maintain cells in a vitreous state at
54 storage temperatures] [9,10]. The hypothesis of water replacement considers that sugars directly
55 interact with the polar heads of lipids in the dried state decreasing the membrane phase transition
56 temperature (T_m). Hence, membranes dehydrated in the presence of sugars remain in the liquid
57 crystalline phase as if they were hydrated [9,10]. These hypotheses are not excluding. On the contrary,
58 it has been reported that in several cases that vitrification is a necessary but not sufficient condition
59 for a good protection. This explains why polysaccharides with high T_g (*i.e.*: maltodextrines, starch)
60 are not good protectants. Moreover, some articles suggest that the conjoint use of high T_g
61 polysaccharides with small sugars having not so high T_g but that interact with membranes (*i.e.*:
62 glucose or sucrose) may be a good protection strategy [4,9].

63 The recovery of desiccated bacteria is an important issue when evaluating the protective
64 capacity of sugars. Therefore, monitoring growth kinetics after rehydrating the dehydrated
65 microorganisms should ideally provide complete information about the evolution of bacteria recovery.
66 *Lag*, exponential (*log*) and stationary phases of growth are characterized by different biochemical
67 reactions leading to the synthesis of the cellular components required for bacteria growth and division
68 [11]. For example, the *log* phase is defined as the balanced growth stage because the average
69 composition of the cells (*i.e.*, protein and DNA) remains constant with bacterial culture properties

1
2
3 70 increasing at the same rate. When the stationary phase is reached, there is no longer a net increase in
4
5 71 viable bacterial cell numbers and cellular metabolic activity is decreased meaning that the growth rate
6
7 72 is equal to that of the death rate. During the transition between *log* and stationary phase, cellular
8
9 73 components are synthesized at unequal rates. For this reason, the biochemical composition of cells in
10
11 74 the stationary phase is different from that in the *log* phase [11]. All these biochemical changes can be
12
13 75 followed in real time using spectroscopic methods [11,12].
14

15
16 76 Methods based on vibrational spectroscopy, including near infrared spectroscopy (NIR) are
17
18 77 particularly useful because of their feasibility for monitoring biological processes without the
19
20 78 necessity of exogenous chemical reagents, which saves costs and time. In addition, the ease to
21
22 79 interface spectroscopic equipments to almost any computer converts NIR in a useful technique for
23
24 80 automatic control, quality assessment or process optimization in real time [13,14]. Spectral features in
25
26 81 NIR provide a rich source of information arising from combinations and overtones of the fundamental
27
28 82 vibrations associated with C-H, O-H and N-H bonds. However, the interpretation of the huge amount
29
30 83 of information contained in the spectra requires the use of chemometric methods. This enables a
31
32 84 dynamic monitoring of industrial processes *in situ*, in environments consisting of complex chemical
33
34 85 mixtures [13,15-17]. In this regard, NIR has been used to detect and monitor microorganisms in food-
35
36 86 related applications [18-31].

37
38 87 Multiparametric flow cytometry (MFC) is a powerful technique that allows discrimination of
39
40 88 microorganisms in different physiological states. The combined use of carboxyfluorescein diacetate
41
42 89 (cFDA) and propidium iodide (PI) probes enables discrimination of viable, dead and damaged cells
43
44 90 [32]. cFDA passively diffuses into cells and intracellular esterases cleave its acetate groups to yield
45
46 91 highly green fluorescent carboxyfluorescein succinimidyl ester. The charged red fluorescent dye PI
47
48 92 labels DNA, but only penetrates bacterial cells with damaged membranes [32].
49

50
51 93 In this work, the role of lactulose and two types of GOS as protectants against dehydration was
52
53 94 evaluated. *Lactobacillus delbrueckii* subsp *bulgaricus* CIDCA 333 was dehydrated in desiccators
54
55 95 containing silica gel until no changes in water desorption were detected. Bacterial growth after
56
57 96 rehydration was followed using NIR and absorbance at 600 nm. Results were interpreted using an
58
59 97 integrated analysis including: a) MFC and b) principal component analysis of the NIR spectra.
60

1
2
3
4
5
6
7
8
9
10
11
12
13
14
15
16
17
18
19
20
21
22
23
24
25
26
27
28
29
30
31
32
33
34
35
36
37
38
39
40
41
42
43
44
45
46
47
48
49
50
51
52
53
54
55
56
57
58
59
60

98

99

MATERIALS AND METHODS

Bacterial strains and growth conditions

Lactobacillus delbrueckii subsp. *bulgaricus* CIDCA 333 was isolated from a fermented product [33]. The strain was stored frozen in 120 g/L non-fat milk solids at -80 °C. Cultures were grown at 37 °C in MRS broth [34].

104

GOS

Two types of GOS containing mixtures of galactose and glucose as monomers were studied: GOS Cup Oligo H-70® (Kowa Company, Tokyo, Japan) kindly donated by Kochi S.A. (Santiago, Chile) and GOS Biotempo, kindly donated by Biocircle Road S.L. (Porto, Portugal). GOS Cup Oligo H-70® contained GOS of different degree of polymerization (DP) whose relative composition was: high-molecular-weight oligosaccharides (DP≥5), 4%; tetrasaccharides (DP 4), 21%; trisaccharides (DP 3), 47%; disaccharides (DP2) and lactose, 23%, and monosaccharides, including glucose and galactose, 5% [7]. The relative composition of GOS Biotempo was: pentasaccharides (DP5), 8%; tetrasaccharides (DP4), 42% and trisaccharides (DP3), 47% [35].

114

Lactulose (4-O-β-D-Galactopyranosyl-(1→4)-β-D-fructofuranose)

Commercial lactulose, disaccharide resulting from isomerization of lactose, was utilized (Discovery fine chemicals, Dorset, UK).

118

Drying over silica gel procedure

One mL cultures in the stationary phase (grown overnight at 37 °C in MRS broth, to attain *ca.* 10⁹ CFU/ mL) were harvested by centrifugation (10 min at 4000 g). The pellets were washed twice with 20% (w/w) solutions of GOS Cup Oligo H-70®, GOS Biotempo and lactulose, previously sterilized using 0.2 μm sterile filters, or with 0.85% w/v sodium chloride (control).

1
2
3 124 The pellets were kept on the centrifuge tubes and dried over desiccators containing silica gel,
4
5 125 until no changes in water desorption were detected as measured gravimetrically (approximately 7
6
7 126 days).

8
9 127

10 11 128 ***Growth kinetics***

12
13 129 Desiccated microorganisms were rehydrated for 15 min at 25 °C in 1 mL of 0.85% (w/v)
14
15 130 sodium chloride. The rehydrated microorganisms were inoculated in 10 mL of MRS broth and
16
17 131 incubated at 37 °C. Growth kinetics were followed by determining:

18
19 132 a) The absorbance at 600 nm every 60 min for each condition assayed.

20
21 133 b) The NIR spectra every 60 min. The spectra were collected *in situ* in the 900-1700 nm
22
23 134 spectral region. An Ocean Optics spectrophotometer (model NIRQuest 512; Dunedin, Florida USA)
24
25 135 equipped with a thermoelectrically cooled charge-coupled device (CCD) in a linear array of 512
26
27 136 pixels (optical resolution: 2 nm; full width at half maximum (FWHM) and signal:noise ratio equal to
28
29 137 15000:1) (Dunedin, Florida USA) was used. NIR absorption spectra were registered under a
30
31 138 transmission configuration, using two optic fibers of low OH content (400 µm of core diameter). One
32
33 139 of them was used to transmit the light towards the sample and other one (addressed to the detector), to
34
35 140 collect the transmitted light. The liquid sample was placed in a quartz cuvette located in a holder
36
37 141 connected to the optical fibers. The integration time for collecting NIR spectra was set at 5 msec and
38
39 142 for each time of incubation, five spectra were registered. As radiation source, a tungsten-Halogen
40
41 143 lamp (model LS-1, Ocean Optics Company) was used. The power output of the lamp (vis/NIR range)
42
43 144 was 6.5 watts. SpectraSuite™ software (Ocean Optics, Dunedin, Florida USA) was used to register
44
45 145 the experimental spectra.

46
47 146

48 49 147 ***Data Analysis***

50
51 148 PCA was performed over the raw NIR spectra using The Unscrambler® software (version 9.8,
52
53 149 CAMO, Norway). The spectra corresponding to the growth kinetics of bacteria desiccated in all
54
55
56
57
58
59
60

1
2
3 150 conditions (with GOS Biotempo, GOS Cup Oligo H-70®, lactulose and without protectants) and
4
5 151 those of the controls were used for the analysis.
6

7 152

9 153 **Flow cytometry analyses**

10
11 154 MFC was used to determine viable, damaged and dead microorganisms throughout each kinetic
12
13 155 of growth. cFDA and PI probes (Molecular Probes, Invitrogen SA, CA, USA) were used according to
14
15 156 Raoult *et al.* (2007) [32]. For each assay, 1 mL of culture was harvested, washed twice and
16
17 157 resuspended in 1 mL milli-Q water. The suspensions were incubated with 1 µl cFDA (50 µg/µL) at 28
18
19 158 °C in the dark for 10 min. Afterwards PI was added to a final concentration of 0.5 mg/mL and
20
21 159 incubated at room temperature for 5 min.
22

23 160 Determinations were carried out with a FACS Calibur instrument using the CellQuest software
24
25 161 (Becton Dickinson, Mountain View, CA, USA) according to Raoult *et al.* (2007) [32]. For each
26
27 162 sample 10,000 events were collected, being the event rate less than 300 events/s. All parameters were
28
29 163 collected as logarithmic signals. FL1 channel (530 nm) was used to set the green fluorescence of
30
31 164 cFDA and FL3 channel (670), to set the red fluorescence of PI. Mixtures of thermally dead cells
32
33 165 (80°C for 30 min) and freshly harvested cells were stained with cFDA and PI both in double-staining
34
35 166 assays. They were used as controls to set the flow cytometer detectors and compensation, to
36
37 167 differentiate four regions: Q1 (dead bacteria): PI+ and cFDA-; Q2 (membrane damaged bacteria): PI+
38
39 168 and cFDA+; Q3 (debris): PI- and cFDA-; and Q4 (viable bacteria): PI- and cFDA+. The percentage of
40
41 169 each population was determined as $[i/(Q1 + Q2 + Q4)] / 100$, where *i* is Q1, Q2, or Q4. No fluorescent
42
43 170 debris (Q3) was excluded [36].
44

45 171

47 172 **Reproducibility of results**

48
49 173 Three sets of experiments performed using three different cultures of microorganisms were
50
51 174 carried out. In each set, samples were prepared in duplicate. The relative differences were
52
53 175 reproducible independently of the set of cultures used. Results obtained for duplicates were also
54
55 176 reproducible.
56

57 177
58
59
60

1
2
3 1784
5 179 **RESULTS**

6
7 180 The plate counts of dehydrated *Lactobacillus delbrueckii* subsp. *bulgaricus* CIDCA 333
8
9 181 immediately after rehydration (time of incubation equal to zero) were: 2.00×10^5 CFU/mL, 6.30×10^4
10
11 182 CFU/mL and 2.00×10^4 CFU/mL for cells desiccated with GOS Biotempo, GOS Cup Oligo H-70®
12
13 183 and lactulose, respectively. Microorganisms desiccated without protective compounds dropped to less
14
15 184 than 10^4 CFU/mL after rehydration.

16
17 185 Figure 1 shows the kinetics of growth of microorganisms desiccated in the presence of GOS
18
19 186 Biotempo, GOS Cup Oligo H-70® and lactulose, followed by absorbance at 600 nm. Microorganisms
20
21 187 dehydrated in the absence of protectants were not able to grow after 30 h of incubation. The efficiency
22
23 188 of the protectants was GOS Biotempo > GOS Cup Oligo H-70® > lactulose, as determined by the
24
25 189 increase of the lag time (15, 20 and 21 h, respectively).

26
27 190 The NIR spectra registered throughout all the kinetics of growth are depicted in Figure 2 (raw
28
29 191 spectra in Scripts I and inverted second derivative spectra in Scripts II). The 1300-1400 nm region
30
31 192 was the most sensitive to the evolution of growth kinetics. In particular, the inverted second derivative
32
33 193 band at ~1370 nm depicted a continuous shift to higher wavenumbers for the control (Figure 2AIII).
34
35 194 On the contrary, no changes were observed for microorganisms dehydrated without protectants,
36
37 195 indicating a correlation between spectral overlap and no growth of microorganisms (Figure 2BIII).
38
39 196 For microorganisms dehydrated with sugars, spectra registered at the beginning of the kinetics fully
40
41 197 overlapped. At intermediate times of incubation, the shift of the ~1370 nm band was gradual, as that
42
43 198 observed in the control. At the end of the kinetics spectral changes were slighter (Figure 2 A,C,D,E
44
45 199 scripts III).

46
47 200 Figure 3 shows more clearly the shift of the ~1370 nm band along with the growth kinetics,
48
49 201 fitting nicely the kinetics of growth depicted in Figure 1 in the lag, log and early stationary phases. In
50
51 202 the late stationary phase, a slight shift of the analyzed band was observed. This shift was only
52
53 203 observed for the controls, which were the only cells that attained the late stationary phase after 30 h of
54
55 204 incubation (see circled squares in Figure 3).
56
57
58
59
60

1
2
3 205 The evolution of viable, dead and damaged cells throughout the kinetics of growth followed a
4
5 206 similar pattern in all the conditions assayed (Figure 4). The relative contribution of viable, damaged
6
7 207 and dead cells in the *lag*, *log* and early stationary phase of growth was mainly determined by the
8
9 208 contribution of viable and damaged cells, as that of dead cells was around 10% (Figures 4A-D). The
10
11 209 contribution of dead cells was higher for microorganisms desiccated without protectants (Figure 4E).

12
13 210 Immediately after rehydration (time equal to zero) cells were mostly damaged. The repair of
14
15 211 that damage, occurring during the *lag* phase, led to a continuous increase of viable cells, which
16
17 212 attained maximum values at the beginning of the *log* phase (70-80% of viable cells in the *log* phase in
18
19 213 all conditions) (Figures 4). These values remained unchanged until the early stationary phase. In the
20
21 214 late stationary phase, damaged and dead cells (that up to that moment remained around 10%) started
22
23 215 increasing at expenses of viable cells. This observation was particularly clear in the controls (Figure
24
25 216 4A), the only cultures that attained the late stationary phase after 30 h of incubation. To obtain a full
26
27 217 picture of the evolution of viable, damaged and dead cells, MFC determinations were followed until
28
29 218 46 h of incubation. This allowed us to obtain information about viable, damaged and dead cells in the
30
31 219 late stationary phase also for desiccated microorganisms.

32
33 220 The differential protectant capacity of GOS and lactulose could also be observed from the MFC
34
35 221 assays. Indeed, the percentage of damaged cells immediately after rehydration (time equal to zero)
36
37 222 was 44, 65 and 76% for cells desiccated with GOS Biotempo, GOS Cup Oligo H-70® and lactulose,
38
39 223 respectively (Figures 4B,C,D).

40
41 224 PCA was carried out over all the NIR spectra registered throughout the five kinetics of growth
42
43 225 (control, cells dehydrated with GOS Biotempo, GOS Cup Oligo H-70® and lactulose, and without
44
45 226 protectants). Figure 5 depicts the PC2 vs PC1 scores plot, where PC1 explains 99% of the total
46
47 227 variance. Three groups were observed along PC1-axis (Figure 5). One of them, containing a high
48
49 228 amount of samples in a quite restricted space along PC1-axis, corresponded to microorganisms in the
50
51 229 *lag* phase (opened circles (*a*) in Figure 5). The second group was the most heterogeneous along PC1-
52
53 230 axis and corresponded to bacteria in *log* phase (opened triangles (*b*) in Figure 5). The third group was
54
55 231 homogeneous along PC1-axis and contained samples in the stationary phase (opened squares (*c*) in
56
57
58
59
60

1
2
3 232 Figure 5). The dash line in the plot separates two groups along PC2-axis, corresponding to situations
4
5 233 where bacteria were mostly **damaged (*d*) or mostly viable (*e*)**. We will come back to this issue in the
6
7 234 Discussion section.

8
9 235

10
11 236

12 13 237 **DISCUSSION**

14
15 238 The use of prebiotics like GOS and lactulose as protective compounds is very recent
16
17 239 [7,8,37,38]. Therefore, for the interpretation of their protectant capacity, several physical chemical
18
19 240 aspects need to be analyzed.

20
21 241 When investigating the efficiency of a given compound as protectant against desiccation, the
22
23 242 recovery of cells after rehydration is an important issue that cannot be underestimated. For this reason,
24
25 243 growth kinetics carried out on desiccated microorganisms are useful to analyze the evolution of this
26
27 244 recovery. In this regard, NIR spectroscopy provided rich information about bacterial recovery after
28
29 245 dehydration-rehydration (Figures 2,3,5). PCA allowed not only the discrimination of microorganisms
30
31 246 in different phases of growth, but also the discrimination related with bacterial damage. The high
32
33 247 percentage of variance explained in PC1-axis (99%) indicated the accuracy of NIR to discriminate
34
35 248 microorganisms in different phases of growth (Figure 5). In particular, the high density of the cluster
36
37 249 corresponding to microorganisms in the *lag* phase indicated the extremely low variability of bacteria
38
39 250 spectra in this phase of growth (Figures 2 and 5). The high overlapping of spectra corresponding to
40
41 251 microorganisms dehydrated without protectants (that did not leave the *lag* phase after 30 h of
42
43 252 incubation) is very graphic in this respect (Figure 2BI). Microorganisms in the stationary phase of
44
45 253 growth also grouped in a dense cluster along PC1-axis, correlating the moderately low variability of
46
47 254 spectra in this phase (Figure 5 group *c*). On the contrary, the higher variability of spectra
48
49 255 corresponding to microorganisms in the exponential phase gave a heterogeneous group along PC1-
50
51 256 axis (Figure 5 group *b*).

52
53
54 257 On the other hand, two groups were observed along PC2-axis, that could be ascribed to
55
56 258 damaged (or dead) and viable cells (Figure 5, groups *d* and *e*). The analysis of MFC supported this
57
58 259 interpretation (Figure 4). In the *log* phase microorganisms were mostly viable (70-80%). This explains
59
60

1
2
3 260 that the heterogeneous group along PC1-axis was very homogeneous along PC2-axis (Figure 5). On
4
5 261 the other hand, damaged cells predominated in the *lag* phase (Figure 4). This explains that cells in this
6
7 262 phase of growth belonged to the damaged group along PC2-axis (Figure 5, groups *b* and *e*). Regarding
8
9 263 microorganisms in the stationary phase, part of them grouped with the damaged cells and part of them
10
11 264 with the viable ones. The co-existence of viable and damaged cells (mostly viable in the early
12
13 265 stationary phase, with an increase of damaged cells in the late stationary phase) explains this
14
15 266 observation (Figures 4 and 5 *c,d,e*). It is important to point out that the slight shift of the second
16
17 267 derivative band at ~1370 nm in the late stationary phase of growth (circled squares in Figure 3), where
18
19 268 damaged and dead cells start increasing (Figure 4A) was a further indication of the physiological
20
21 269 information provided by NIR spectroscopy. All these observations reinforce the usefulness of NIR to
22
23 270 easily obtain physiological information in real time without the need of exogenous reagents.

24
25 271 The information provided by MFC assays also explained the different protectant capacity of
26
27 272 both GOS and lactulose. If considered that once attained the *log* phase, bacteria are mostly viable
28
29 273 (about 70-80% in all cases, including controls) and that it is during the *lag* phase when
30
31 274 microorganisms repair their damage (damaged cells decreased during this phase of growth in all
32
33 275 conditions) (Figure 4), one can logically conclude that the length of the *lag* phase was determined by
34
35 276 the decrease of damaged cells during the *lag* phase. This decrease is conditioned by the percentage of
36
37 277 damaged cells immediately after rehydration (time equal to zero). Hence, the lower the percentage of
38
39 278 damaged cells after rehydration, the lower the time required to repair them. In this regard, after
40
41 279 rehydrating microorganisms desiccated with GOS Biotempo, GOS Cup Oligo H-70® and lactulose,
42
43 280 the percentage of damage was 44, 65 and 76%, respectively (Figures 4B,C,D). This supports the
44
45 281 greater protectant capacity of GOS Biotempo (shorter *lag* time) (Figure 1, 3 and 4). The short *lag* time
46
47 282 observed for the controls (containing 20% of damaged cells at time equal to 0) gives further support to
48
49 283 this observation.

50
51 284 The higher T_g of GOS Biotempo with regard to GOS Cup Oligo H-70® and lactulose can
52
53 285 explain their greater protectant capacity on the light of the vitrification hypothesis of preservation
54
55 286 [38]. The different composition of GOS Biotempo and GOS Cup Oligo H-70® provides further
56
57
58
59
60

1
2
3 287 information for the interpretation of their protectant mechanisms. GOS Biotempo were obtained after
4
5 288 removing mono and disaccharides from the whole mixtures of oligosaccharides, whereas GOS Cup
6
7 289 Oligo H-70® not [35]. This results in: a) a higher content of DP3 and DP4 in GOS Biotempo and b)
8
9 290 the presence of mono and disaccharides in GOS Cup Oligo H-70®. Considering the water
10
11 291 replacement hypothesis of preservation, one can conjecture that the higher content of larger
12
13 292 oligosaccharides (DP3 and DP4) allows a stronger interaction with polar head groups [9]. Considering
14
15 293 that vitrification is necessary but not sufficient to explain protection, this explanation seems to be
16
17 294 plausible.

18
19 295 In this regard, Crowe *et al.* (1998) reported that the effect of sugars on depressing T_m can be
20
21 296 determined by their size [9]. In fact, raffinose is more effective than trehalose and this sugar, more
22
23 297 effective than glucose in decreasing T_m of dipalmitoyl phosphatidylcholine (DPPC) membranes [9].
24
25 298 Hinch *et al.* (2003) carried out a systematic study on the stabilization of egg phosphatidylcholine
26
27 299 (EPC) membranes by raffinose family of sugars, including sucrose (DP2), raffinose (DP3), stachyose
28
29 300 (DP4) and verbascose (DP5) [39]. They found that these sugars prevent fusion and leakage of EPC
30
31 301 liposomes progressively better with increasing the DP. This stabilization was explained on the basis of
32
33 302 the greater capacity of higher DP sugars to interact with lipid membranes (depressing T_m), and also to
34
35 303 their higher T_g [39].

36
37 304 In GOS Cup Oligo H-70®, the presence of mono and disaccharides, together with
38
39 305 oligosaccharides of greater DP, also has a vitrification effect, although lower than in GOS Biotempo
40
41 306 [8,35,38]. Moreover, mono and disaccharides interact with membranes in a lesser extent than DP3 [9].
42
43 307 Cells dehydrated with lactulose were the most damaged after rehydration (76%; Figure 4). Lactulose
44
45 308 is mainly known as prebiotic, and their physical chemical properties have never been addressed.
46
47 309 According to the present results, the lower protective capacity could be explained on the basis of a
48
49 310 lower vitrification capacity [38], but further studies are necessary to assess the interaction of lactulose
50
51 311 with lipid membranes.
52
53
54
55
56 312
57 313
58
59
60

1
2
3 314 **CONCLUSIONS**

4
5 315 The impact of the obtained results can be considered from two main perspectives: a) the
6
7 316 usefulness of NIR to provide complete information about bacterial physiology during growth kinetics;
8
9 317 b) the efficiency of GOS and lactulose as bacterial protectants during dehydration.

10
11 318 The repair of bacterial damage resulting from dehydration is critical for starter fermentation.
12
13 319 Registration of NIR spectra is as simple as turbidimetric determinations, but has the enormous
14
15 320 advantage of providing information about physiological state of cells. In this sense, the possibility of
16
17 321 following the evolution of viable cells in a quick and non-invasive way strongly supports the use of
18
19 322 NIR for monitoring starter fermentation at an industrial level.

20
21 323 The protectant capacity of prebiotics like GOS and lactulose during freeze-drying has been
22
23 324 addressed for the first time in the last years [7,8,37,38]. In this work, we provided an insight on their
24
25 325 protection capacity against dehydration. The greater contribution of DP3 and DP4 in the composition
26
27 326 of GOS Biotempo can explain their better protectant capacity on the basis of the vitrification
28
29 327 hypothesis of preservation. Considering previous works carried out on related oligosaccharides, an
30
31 328 interaction with polar head lipid membranes cannot be discharged, thus reinforcing the protectant
32
33 329 capacity of GOS Biotempo [9,39].

34
35
36 330

37 331 **Acknowledgments**

38
39 332 This work was supported by the Argentinean Agency for the Scientific and Technological
40
41 333 Promotion (Projects PICT/2008/145 and PICT/2011/0226), the Argentinean National Research
42
43 334 Council (CONICET) (PIP2012-2014114-201101-00024), the Mexican PIFI/UAZ/2012-program, the
44
45 335 Mexican National Research Council (CONACyT) [Project No. 153066 (2010)], and the bilateral
46
47 336 project CONACyT-MINCYT (México, Argentina) (163687/208443; Mx11/01). Authors acknowledge
48
49 337 D. Torres for providing GOS Biotempo and L. Delgadillo-Ruiz for technical assistance. AGZ and
50
51 338 EET are members of the research career CONICET. MIS is doctoral fellow from CONICET.

52
53
54 339

55
56 340 **Competing Interests:** The authors declare that they have no competing interests.
57
58
59
60

341 **REFERENCES**

- 342 1. Tymczyszyn EE, Gómez-Zavaglia A, Disalvo EA. Effect of sugars and growth media on the
343 dehydration of *Lactobacillus delbrueckii* ssp. *bulgaricus*. *J. Appl. Microbiol.* 2007;102:845-851.
- 344 2. Tymczyszyn EE, Díaz MR, Pataro A, Sandonato N, Gómez-Zavaglia A, Disalvo EA. Critical
345 water activity for the preservation of *Lactobacillus bulgaricus* by vacuum drying *Int J Food*
346 *Microbiol.* 2008;128:342-347.
- 347 3. Fonseca F, Béal C, Mihoub F, Marin M, Corrieu G. Improvement of cryopreservation of
348 *Lactobacillus delbrueckii* subsp. *bulgaricus* CFL1 with additives displaying different protective
349 effects. *Int Dairy J.* 2003;13:917-926.
- 350 4. Oldenhof H, Wolkers W, Fonseca F, Passot S, Marin M. Effect of sucrose and maltodextrin on
351 the physical properties and survival of air-dried *Lactobacillus bulgaricus*: an *in situ* Fourier
352 transform infrared spectroscopy study. *Biotechnol Prog.* 2005;21:885-892.
- 353 5. Santivarangkna C, Higl B, Foerst P. Protection mechanisms of sugars during different stages of
354 preparation process of dried lactic acid starter cultures. *Food Microbiol.* 2008;25:429-441.
- 355 6. Golowczyc MA, Gerez CL, Silva J, Abraham AG, De Antoni GL, Teixeira PM. Survival of
356 spray-dried *Lactobacillus kefir* is affected by different protectants and storage conditions.
357 *Biotechnol Lett.* 2011;33:681-686.
- 358 7. Tymczyszyn EE, Gerbino E, Illanes A, Gómez-Zavaglia A. Galacto-oligosaccharides as
359 protective molecules in the preservation of *Lactobacillus delbrueckii* subsp. *bulgaricus*.
360 *Cryobiology.* 2011;62:123-129.
- 361 8. Tymczyszyn EE, Sosa N, Gerbino E, Gómez-Zavaglia A, Schebor C. Effect of physical
362 properties on the stability of *Lactobacillus bulgaricus* in a freeze-dried galacto-oligosaccharides
363 matrix. *Int J Food Microbiol.* 2012;155:217-221.
- 364 9. Crowe JH, Carpenter JF, Crowe LM. The role of vitrification in anhydrobiosis. *Annu Rev*
365 *Physiol.* 1998;60:73-103.
- 366 10. Crowe JW, Hoekstra FA, Crowe LM. Anhydrobiosis. *Annu Rev Physiol.* 1992;54:570-599.
- 367 11. Al-Qadiri HM, Alami NI, Al-Holy MA, Lin M, Cavinato AG, Rasco BA. *J Rapid Meth Aut Mic.*
368 2008;16:73-89.

- 1
2
3 369 12. Harz M, Rösch P, Popp J. Vibrational spectroscopy-A powerful tool for the rapid identification
4
5 370 of microbial cells at the single-cell level. *Cytometry*. 2009;75A:104-113.
6
7 371 13. Cervera AE, Petersen N, Lantz AE, Larsen A, Gernaey KV. Application of near-infrared
8
9 372 spectroscopy for monitoring and control of cell culture and fermentation. *Biotechnol Prog*.
10
11 373 2009;25:1561-1581.
12
13 374 14. McClure FW. 204 years of near infrared technology: 1800-2003. *J Near Infrared Spec*.
14
15 375 2003;11:487-518.
16
17 376 15. Bonanno AS, Olinger JM, Griffiths PR. The origin of band positions and widths in near infrared
18
19 377 spectra. In: Hildrum KI, Isaakson T, Naes T, Tandberg, A. Near infrared spectroscopy: bridging
20
21 378 the gap between data analysis and NIR applications. London: Ellis Horwood. 1992:19-28.
22
23 379 16. Small GW. Chemometrics and near-infrared spectroscopy: avoiding the pitfalls. *Trend Anal*
24
25 380 *Chem*. 2006;25:1057-1066.
26
27 381 17. Zhang L, Small GW, Arnold MA. Calibration standardization algorithm for partial least-squares
28
29 382 regression: application to the determination of physiological levels of glucose by near-infrared
30
31 383 spectroscopy. *Anal Chem*. 2002;74:4097-4108.
32
33 384 18. Vaccari G, Dosi E, Campi AL, González-Vera A, Matteuzzi R, Mantovani G. A near-infrared
34
35 385 spectroscopy technique for the control of fermentation processes: An application to lactic acid
36
37 386 fermentation. *Biotechnol Bioeng*. 1993;43:913-917.
38
39 387 19. Sivakesava S, Irudayaraj J, Ali D. Simultaneous determination of multiple components in lactic
40
41 388 acid fermentation using FT-MIR, NIR, and FT-Raman spectroscopic techniques. *Process*
42
43 389 *Biochem*. 2001;37:371-378.
44
45 390 20. Rodriguez-Saona L, Khambaty F, Fry F, Calvey E. Rapid detection and identification of bacterial
46
47 391 strains by Fourier transform near infrared spectroscopy. *J Agric Food Chem*. 2001;49:574-579.
48
49 392 21. Arnold SA, Gaensakoo R, Harvey LM, McNeil B. Use of at-line and *in situ* near infrared
50
51 393 spectroscopy to monitor biomass in an industrial fed-batch *Escherichia coli* process. *Biotechnol*
52
53 394 *Bioeng*. 2002;80:405-413.
54
55 395 22. Cimander C, Carlsson M, Mandenius CF. Sensor fusion for on-line monitoring of yoghurt
56
57 396 fermentation. *J Biotechnol*. 2002;99:237-248.
58
59
60

- 1
2
3 397 23. Macedo MG, Laporte MF, Lacroix C. Quantification of exopolysaccharide, lactic acid, and
4
5 398 lactose concentrations in culture broth by near-infrared spectroscopy. *J Agric Food Chem.*
6
7 399 2002;50:1774-1779.
8
9 400 24. Tamburini E, Vaccari G, Tosi S, Trilli A. Near-infrared spectroscopy: a tool for monitoring
10
11 401 submerged fermentation processes using an immersion optical-fiber probe. *Appl Spectrosc.*
12
13 402 2003;57:132-138.
14
15 403 25. Tosi S, Rossi M, Tamburini E, Vaccari G, Amaretti A, Matteuzzi D. Assessment of in-line near
16
17 404 infrared spectroscopy for continuous monitoring of fermentation processes. *Biotechnol Prog.*
18
19 405 2003;19:1816-1821.
20
21 406 26. Navrátil M, Cimander C, Mandenius CF. On-line multisensor monitoring of yogurt and filmjölök
22
23 407 fermentations on production scale. *J Agric Food Chem.* 2004;52:415-420.
24
25 408 27. Saranwong S, Kawano S. System design for non-destructive near infrared analyses of chemical
26
27 409 components and total aerobic bacteria count of raw milk. *J Near Infrared Spec.* 2008;16:389-
28
29 410 398.
30
31 411 28. Saranwong S, Kawano S. Interpretation of near infrared calibration structure for determining the
32
33 412 total aerobic bacteria count in raw milk: interaction between bacterial metabolites and water
34
35 413 absorptions. *J Near Infrared Spec.* 2008;16:497-504.
36
37 414 29. Cámara-Martos F, Zurera-Cosano G, Moreno-Rojas R, García-Gimeno RM, Pérez-Rodríguez F.
38
39 415 Identification and quantification of lactic acid bacteria in a water-based matrix with near-infrared
40
41 416 spectroscopy and multivariate regression modeling. *Food Anal Method.* 2012;5:19-28.
42
43 417 30. Feng YZ, ElMasry G, Sun DW, Scannell AGM, Walsh D, Morcy N. Near-infrared hyperspectral
44
45 418 imaging and partial least squares regression for rapid and reagentless determination of
46
47 419 Enterobacteriaceae on chicken fillets. *Food Chem.* 2013;138:1829-1836.
48
49 420 31. Goldfeld M, Christensen J, Pollard D, Gibson ER, Olesberg JT, Koerperick EJ, Lanz K, Small
50
51 421 GW, Arnold MA, Evans CE. Advanced near-infrared monitor for stable real-time measurement
52
53 422 and control of *Pichia pastoris* bioprocesses. *Biotechnol Prog.* 2014;30:749-759.
54
55
56
57
58
59
60

- 1
2
3 423 **32.** Rault A, Béal C, Ghorbal S, Ogier JC, Bouix M. Multiparametric flow cytometry allows rapid
4 424 assessment and comparison of lactic acid bacteria viability after freezing and during frozen
5 425 storage. *Cryobiology*. 2007;55:35-43.
- 6
7
8
9 426 **33.** Gómez-Zavaglia A, Abraham A, Giorgieri S, De Antoni GL. Application of polyacrylamide gel
10 427 electrophoresis and capillary gel electrophoresis to the analysis of *Lactobacillus delbrueckii*
11 428 whole-cell proteins. *J Dairy Sci*. 1999;82:870-877.
- 12
13
14
15 429 **34.** De Man JO, Rogosa M, Sharpe ME. A medium for the cultivation of lactobacilli. *J Appl*
16 430 *Bacteriol*. 1960;23:130-135.
- 17
18
19 431 **35.** Torres DPM, Bastos M, Goncalves MPF, Teixeira JA, Rodrigues LR. Water sorption and
20 432 plasticization of an amorphous galacto-oligosaccharide mixture. *Carbohydr Polym*. 2011;83:831-
21 433 835.
- 22
23
24
25 434 **36.** Hiraoka Y, Kimbara K. Rapid assessment of the physiological status of the polychlorinated
26 435 biphenyl degrader *Comamonas testosteroni* TK102 by flow cytometry. *Appl Environ Microbiol*.
27 436 2002;68:2031-2035.
- 28
29
30
31 437 **37.** Golowczyc M, Vera C, Santos M, Guerrero C, Carasi P, Illanes A, Gómez-Zavaglia A,
32 438 Tymczyszyn EE. Use of whey permeate containing in situ synthesized galacto-oligosaccharides
33 439 for the growth and preservation of *Lactobacillus plantarum*. *J Dairy Res*. 2013;80:374-381.
- 34
35
36
37 440 **38.** Santos M, Gerbino E, Araujo-Andrade C, Tymczyszyn EE, Gomez-Zavaglia A. Stability of
38 441 freeze-dried *Lactobacillus delbrueckii* subsp. *bulgaricus* in the presence of galacto-
39 442 oligosaccharides and lactulose as determined by near infrared spectroscopy. *Food Res Int*.
40 443 2014;59:53-60.
- 41
42
43
44
45 444 **39.** Hinch DK, Zuther E, Heyer AG. The preservation of liposomes by raffinose family
46 445 oligosaccharides during drying is mediated by effects on fusion and lipid phase transitions.
47 446 *Biochim Biophys Acta*. 2003;1612:172-177.
- 48
49
50
51 447

448 **CAPTIONS TO FIGURES**

449

450 **Figure 1:** Growth kinetics of *Lactobacillus delbrueckii* subsp. *bulgaricus* CIDCA 333 dehydrated in
451 the presence of GOS Biotempo (opened up triangles), GOS Cup Oligo-H70® (opened
452 circles), and lactulose (opened down triangles). Controls: non-dehydrated microorganisms
453 (full black squares); microorganisms dehydrated without sugar (full gray squares). Kinetics
454 were followed by determining absorbance at 600 nm.

455 **Figure 2:** Growth kinetics of *Lactobacillus delbrueckii* subsp. *bulgaricus* CIDCA 333 followed by
456 NIR. Arrows indicate the beginning (time equal to zero) and the end (time equal to 30 h) of
457 the growth kinetics. (A) Control (non dehydrated microorganisms); (B) Microorganisms
458 dehydrated without protectant; (C) Microorganisms dehydrated in the presence of GOS
459 Biotempo; (D) Microorganisms dehydrated in the presence of GOS Cup Oligo H-70®; (E)
460 Microorganisms dehydrated in the presence of lactulose.

461 Srippts I: normalized raw spectra; Srippts II: normalized second derivative spectra (inverted
462 spectra are shown); Script III: normalized second derivative spectra in the 1350-1400 nm
463 region (inverted spectra are shown).

464 **Figure 3:** Position of the inverted second derivative band at ~1370 nm as a function of the time of
465 incubation. Microorganisms dehydrated with GOS Biotempo (opened up triangles), GOS
466 Cup Oligo-H70® (opened circles), and lactulose (opened down triangles). Controls: non-
467 dehydrated microorganisms (full black squares); microorganisms dehydrated without sugar
468 (full gray squares). Circled symbols correspond to microorganisms in the late stationary
469 phase.

470 **Figure 4:** Evolution of viable, damaged and dead microorganisms throughout the kinetics of growth.
471 (A) Control (non dehydrated microorganisms); (B) Microorganisms dehydrated with GOS
472 Biotempo; (C) Microorganisms dehydrated with GOS Cup Oligo H-70®; (D)
473 Microorganisms dehydrated with lactulose; (E) Microorganisms dehydrated without

1
2
3 474 protectant; Full squares, opened triangles and opened circles denote viable, damaged and
4
5 475 dead microorganisms, respectively.
6

7 476 **Figure 5:** Scores plot from the PCA carried out on the NIR spectra of *Lactobacillus delbrueckii*
8
9 477 subsp. *bulgaricus* CIDCA 333 in different phases of growth. The spectra registered
10
11 478 throughout all the kinetics of growth (controls and microorganisms dehydrated with the
12
13 479 three sugars and without protectants) were considered for the analysis. Circles denote
14
15 480 microorganisms in the *lag* phase, triangles, microorganisms in the *log* phase and squares,
16
17 481 microorganisms in the stationary phase. Letters *a*, *b* and *c* denote microorganisms in the *lag*,
18
19 482 *log* and stationary phase of grow; letters *c* and *d*, denote viable and damaged cells. The dash
20
21 483 line separates groups *c* and *d* (viable and damaged cells).
22
23
24
25
26
27
28
29
30
31
32
33
34
35
36
37
38
39
40
41
42
43
44
45
46
47
48
49
50
51
52
53
54
55
56
57
58
59
60

1
2
3
4
5
6
7
8
9
10
11
12
13
14
15
16
17
18
19
20
21
22
23
24
25
26
27
28
29
30
31
32
33
34
35
36
37
38
39
40
41
42
43
44
45
46
47
48
49
50
51
52
53
54
55
56
57
58
59
60

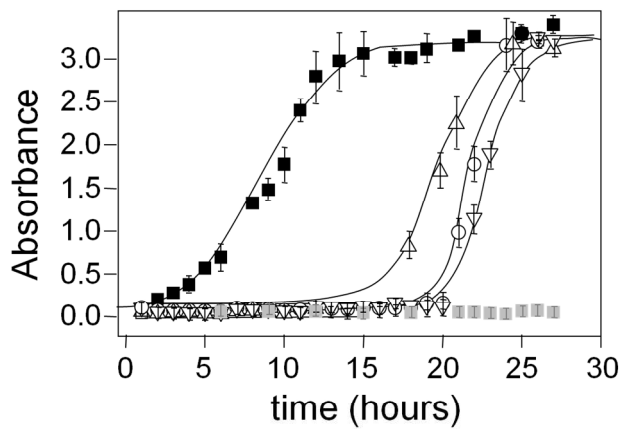
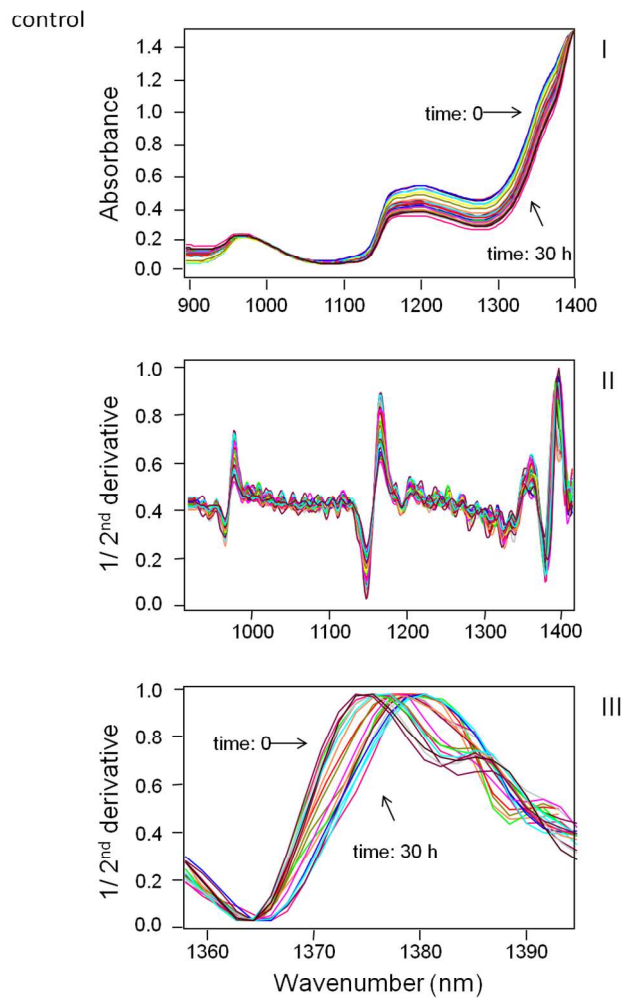


Figure 1

Figure 1
297x209mm (300 x 300 DPI)

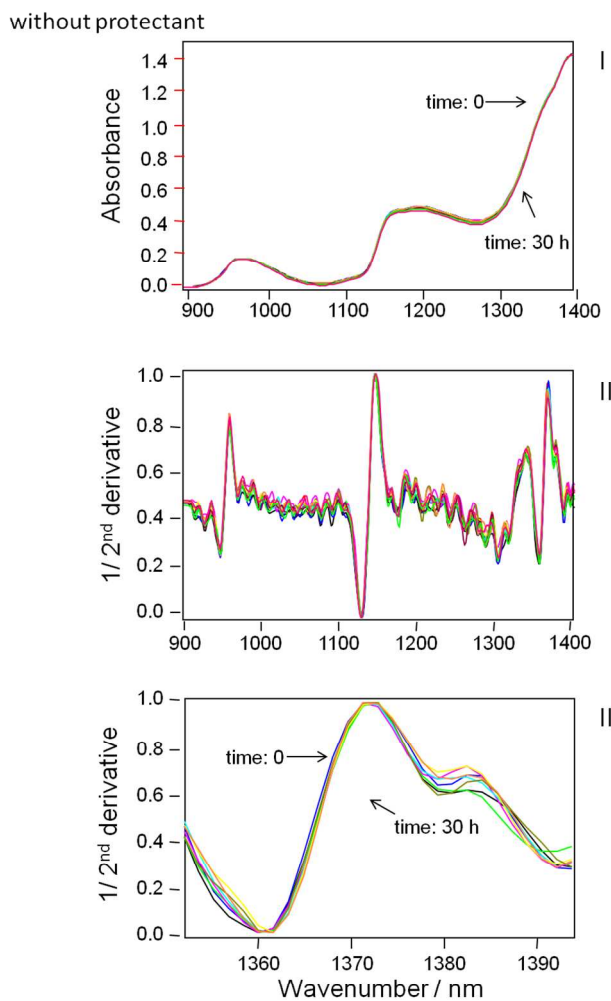
1
2
3
4
5
6
7
8
9
10
11
12
13
14
15
16
17
18
19
20
21
22
23
24
25
26
27
28
29
30
31
32
33
34
35
36
37
38
39
40
41
42
43
44
45
46
47
48
49
50
51
52
53
54
55
56
57
58
59
60



A

Figure 2

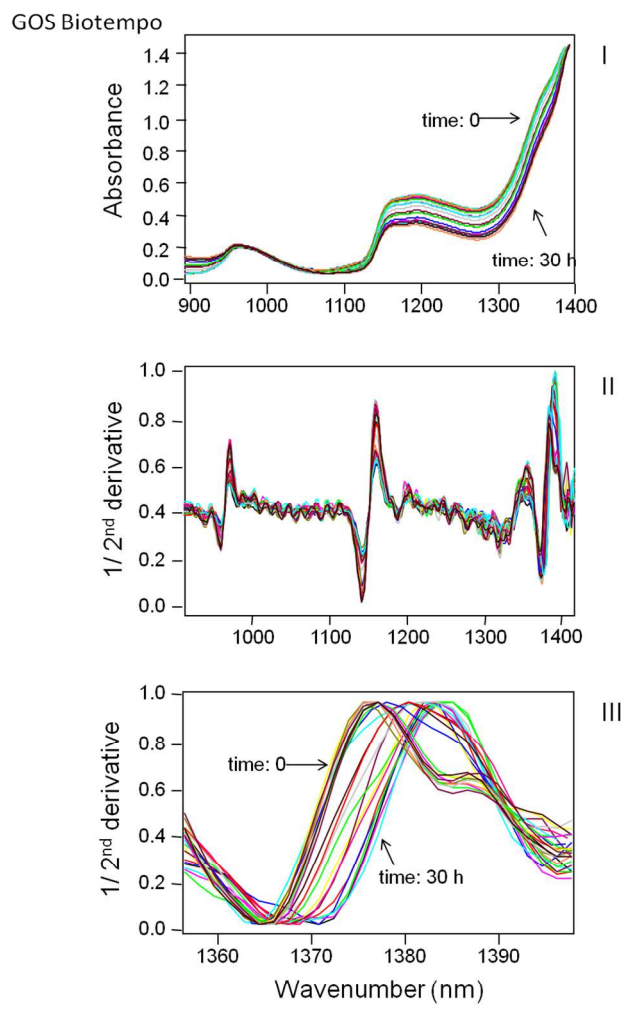
209x297mm (300 x 300 DPI)



209x297mm (300 x 300 DPI)

1
2
3
4
5
6
7
8
9
10
11
12
13
14
15
16
17
18
19
20
21
22
23
24
25
26
27
28
29
30
31
32
33
34
35
36
37
38
39
40
41
42
43
44
45
46
47
48
49
50
51
52
53
54
55
56
57
58
59
60

1
2
3
4
5
6
7
8
9
10
11
12
13
14
15
16
17
18
19
20
21
22
23
24
25
26
27
28
29
30
31
32
33
34
35
36
37
38
39
40
41
42
43
44
45
46
47
48
49
50
51
52
53
54
55
56
57
58
59
60

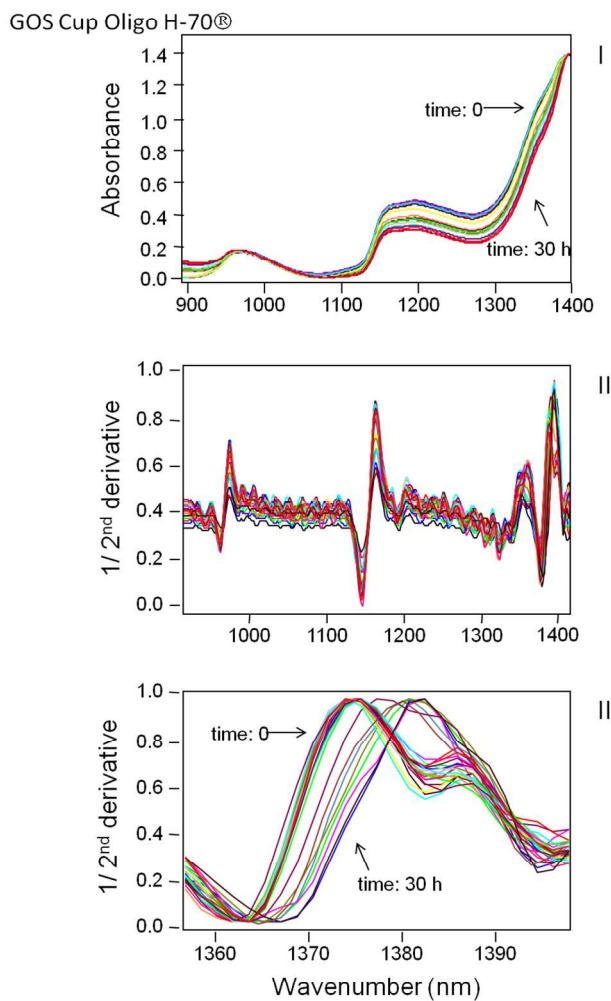


C

Figure 2

209x297mm (300 x 300 DPI)

1
2
3
4
5
6
7
8
9
10
11
12
13
14
15
16
17
18
19
20
21
22
23
24
25
26
27
28
29
30
31
32
33
34
35
36
37
38
39
40
41
42
43
44
45
46
47
48
49
50
51
52
53
54
55
56
57
58
59
60



D

Figure 2

209x297mm (300 x 300 DPI)

1
2
3
4
5
6
7
8
9
10
11
12
13
14
15
16
17
18
19
20
21
22
23
24
25
26
27
28
29
30
31
32
33
34
35
36
37
38
39
40
41
42
43
44
45
46
47
48
49
50
51
52
53
54
55
56
57
58
59
60

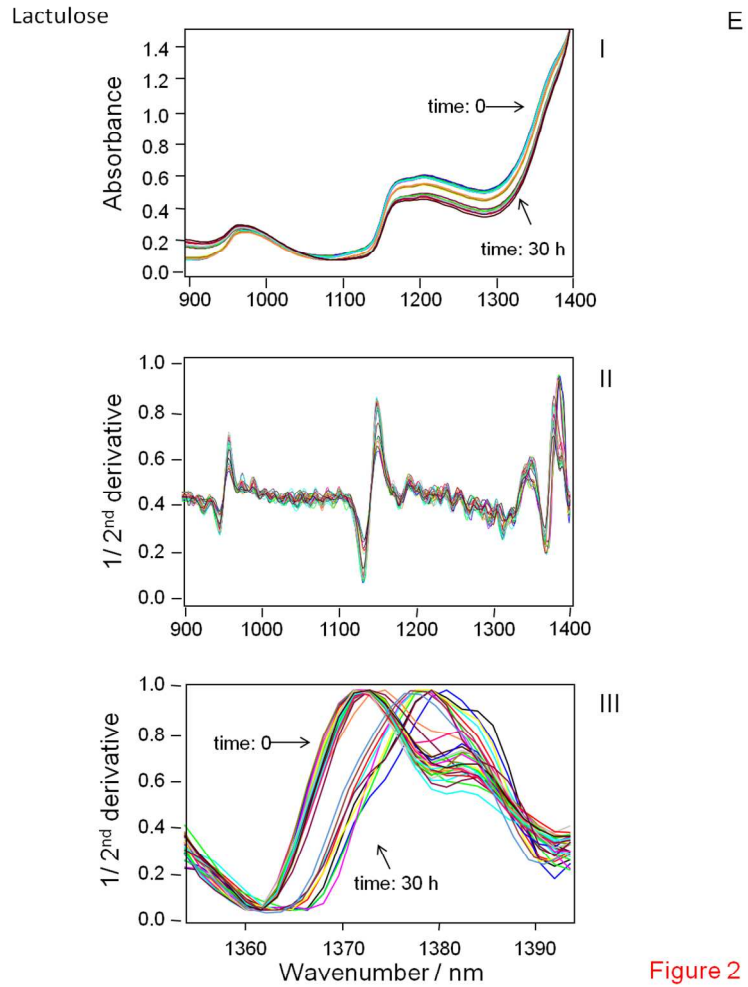


Figure 2

209x297mm (300 x 300 DPI)

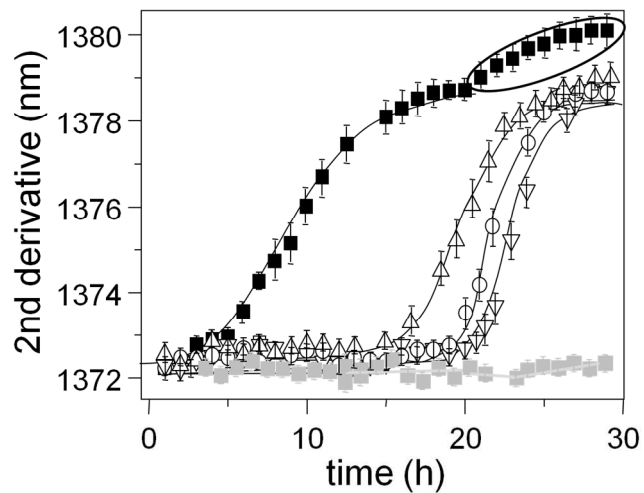


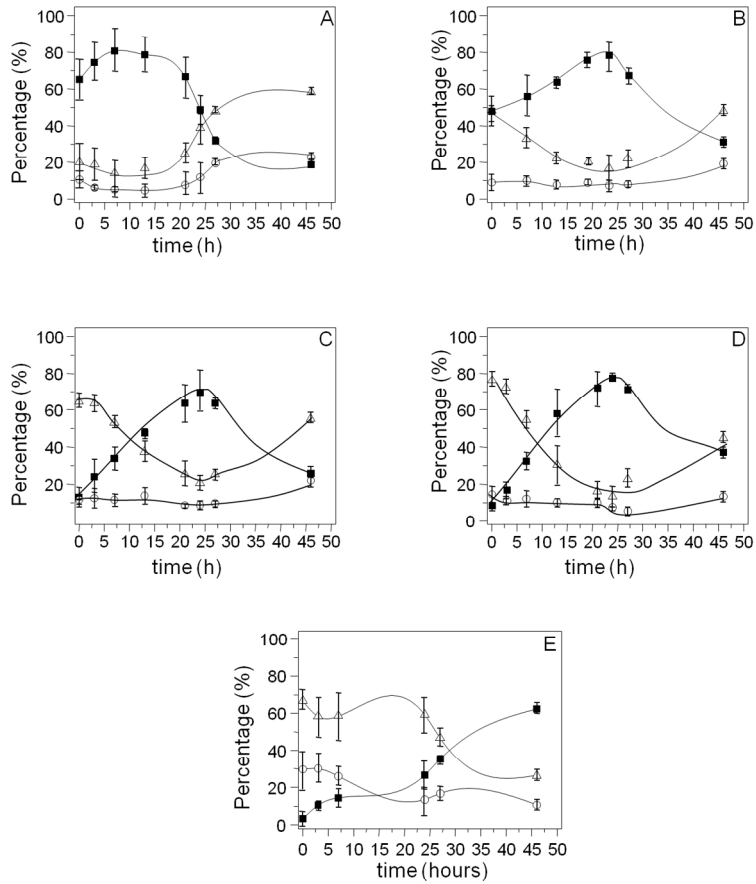
Figure 3

297x209mm (300 x 300 DPI)

Review

1
2
3
4
5
6
7
8
9
10
11
12
13
14
15
16
17
18
19
20
21
22
23
24
25
26
27
28
29
30
31
32
33
34
35
36
37
38
39
40
41
42
43
44
45
46
47
48
49
50
51
52
53
54
55
56
57
58
59
60

1
2
3
4
5
6
7
8
9
10
11
12
13
14
15
16
17
18
19
20
21
22
23
24
25
26
27
28
29
30
31
32
33
34
35
36
37
38
39
40
41
42
43
44
45
46
47
48
49
50
51
52
53
54
55
56
57
58
59
60



209x297mm (300 x 300 DPI)

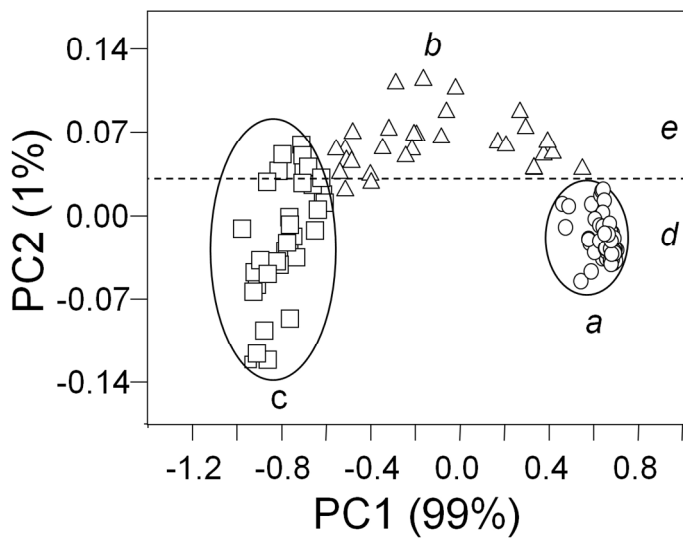


Figure 5

297x209mm (300 x 300 DPI)

Review

1
2
3
4
5
6
7
8
9
10
11
12
13
14
15
16
17
18
19
20
21
22
23
24
25
26
27
28
29
30
31
32
33
34
35
36
37
38
39
40
41
42
43
44
45
46
47
48
49
50
51
52
53
54
55
56
57
58
59
60